Piezoelectric control of a machine tool with parallel kinematics

Christian Rudolf [a], Jörg Wauer [a], Christian Munzinger [b] and Martin Weis [b]

[a] Institut für Technische Mechanik,   [b] Institut für Produktionstechnik,
Universität Karlsruhe (TH), Kaiserstr. 12, 76128 Karlsruhe, Germany

ABSTRACT

An adaptronic strut, developed for compensation of the influence of geometric faults in machine tools with parallel kinematic structure, is examined. A simple oscillator model of the strut is built. First, the equations of motions for this simplified model are derived analytically. These information are used for designing a single variable state control based on the principles of the optimal least quadratic regulator (LQR). Afterwards, the controller concept is extended applying an additional PI-controller. Secondly, the strut is modeled using the commercial multi-body system simulation software MSC.ADAMS. The required system state which is not explicitly given within MSC.ADAMS primarily has to be estimated. For this task a LUENBERGER observer is implemented. A similar single variable state control is developed and both designs are compared among themselves when the adaptronic strut is examined under external loads. Finally, the strut is implemented into the model of the complete machine tool and its influence on the behavior of the machine tool is treated.

Keywords: Machine tools, parallel kinematics, adaptronic state control, LQR, LUENBERGER observer

1. INTRODUCTION

Machine tools with parallel kinematic structure recommend themselves due to their stiffness and dynamics. However, due to geometric faults in parts of the machine tool, such as differing geometries resulting, for example, from production tolerances and assembly errors, stresses within the structure occur. These stresses can lead to deflections of the tool center point (TCP), reducing the quality of the workpiece. In addition, machine tools with ideally three translational degrees of freedom, as shown exemplarily in Fig. 1, exhibit a full three-dimensional behavior. Translational deflections can be compensated by additional movement of the guiding skids, for the compensation of rotational deflections the adaptronic strut shown in Fig. 2 was developed. The strut is similar
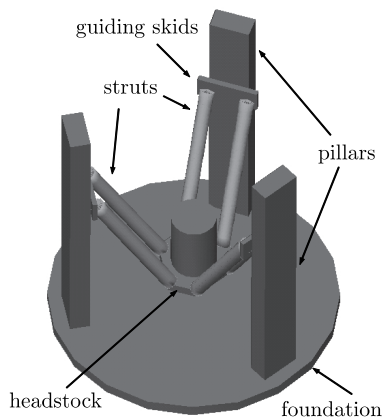
Figure 1. Parallel kinematic machine tool with three translational degrees of freedom.
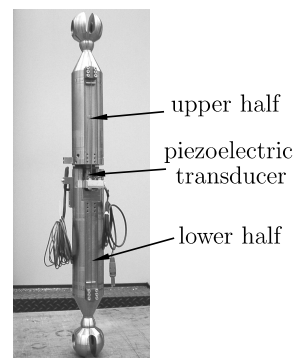
Figure 2. Adaptronic strut[1].

[a] Send correspondence to: rudolf@itm.uni-karlsruhe.de

in shape to a general strut in machine tools separated in two halves with a piezoelectric transducer unit placed in-between. For the model considered within this paper this description is sufficient. The additionally required components as well as the complete functional principle of the strut is described in[1–3].

2. PHYSICAL MODEL

For designing a state controller, in a first step the adaptronic strut can be reduced to a simple oscillator with three masses as shown in Fig. 3. The lower and upper half of the strut are represented by masses m_1 and
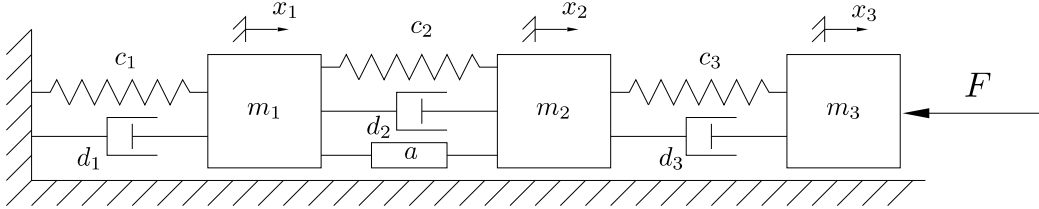
Figure 3. Oscillator with three masses.

m_3, respectively, the piezoelectric transducer is represented by mass m_2. The positions of the three bodies are described by the corresponding coordinates x_i ($i \in \{1, 2, 3\}$). The stiffness coefficients c_i can be calculated to $c_i = \frac{E_i A_i}{\ell_i}$ using HOOKES LAW $\frac{F}{A} = \sigma = E\varepsilon = E\frac{\Delta\ell}{\ell}$, with YOUNG's Modulus E_i, approximated cross-sectional area A_i and length ℓ_i of the three parts of the adaptronic strut. The material damping is described by approximated parameters d_i. The system experiences the influence of the external disturbance load F, representing 'process loads' and it is controlled by the piezoelectric transducer, whose actuating force F_r is acting on body m_2 and reacting on body m_1. Within this contribution we concentrate on the actuating force and only marginally consider the dependency between the actuator force F_r and the required voltage U. For low voltage signals the linear piezoelectric constitutive equations

$$\begin{align} T_p &= c_{pq}^E S_q - e_{kp} E_k \tag{1} \\ D_i &= e_{iq} S_q + \varepsilon_{ik}^S E_k \tag{2} \end{align}$$

apply with T_p and S_q being stress and strain in the piezoelectric material and E_k and D_i being the electric field and the electric displacement. Thus, for a stack actuator the force due to the applied voltage U then is $F_r = kU$, where k is an abbreviation for geometry and material properties of the actuator[1]. In case of large voltage signals the hysteretic dependency between actuator voltage and actuator force can be described using elementary superposition, hysteresis and creep operators, whose non-linear influence can be compensated by inverse control, see Kuhnen et al.[4–6].

2.1. Analytical description

Written in matrix form the equations of motion of the system shown in Fig. 3 read

$$\boldsymbol{M}\ddot{\boldsymbol{x}} + \boldsymbol{D}\dot{\boldsymbol{x}} + \boldsymbol{C}\boldsymbol{x} = \boldsymbol{f}F_r + \boldsymbol{f}_S F \tag{3}$$

with vectors $\boldsymbol{x} = [x_1, x_2, x_3]^T$, $\boldsymbol{f} = [-1, 1, 0]$ and $\boldsymbol{f}_S = [0, 0, -1]^T$, as well as mass matrix $\boldsymbol{M} = \mathrm{diag}(m_i)$, damping matrix $\boldsymbol{D}$ and stiffness matrix $\boldsymbol{C}$, where

$$\boldsymbol{D} = \begin{bmatrix} d_1 + d_2 & -d_2 & 0 \\ -d_2 & d_2 + d_3 & -d_3 \\ 0 & -d_3 & d_3 \end{bmatrix} \text{ and } \boldsymbol{C} = \begin{bmatrix} c_1 + c_2 & -c_2 & 0 \\ -c_2 & c_2 + c_3 & -c_3 \\ 0 & -c_3 & c_3 \end{bmatrix} \tag{4}$$

with coefficients d_i such that the convenience hypothesis $\boldsymbol{D} = \alpha \boldsymbol{M} + \beta \boldsymbol{C}$ is fulfilled.

Introducing the state variable vector $\boldsymbol{z}^T = [\dot{\boldsymbol{x}}^T, \boldsymbol{x}^T]$, the equations of motion (3) can be rewritten in state space form

$$\dot{\boldsymbol{z}} = \boldsymbol{A}\boldsymbol{z} + \boldsymbol{b}\, u + \boldsymbol{b}_S\, u_S \tag{5}$$

with

$$\boldsymbol{A} = \begin{bmatrix} -\boldsymbol{M}^{-1}\boldsymbol{D} & -\boldsymbol{M}^{-1}\boldsymbol{C} \\ \boldsymbol{I} & \boldsymbol{0} \end{bmatrix}, \quad \boldsymbol{b} = \begin{bmatrix} \boldsymbol{M}^{-1}\boldsymbol{f} \\ \boldsymbol{0} \end{bmatrix}, \quad \boldsymbol{b}_S = \begin{bmatrix} \boldsymbol{M}^{-1}\boldsymbol{f}_S \\ \boldsymbol{0} \end{bmatrix}. \tag{6}$$

In the system considered the plant output shall be the position x_3 of mass m_3. Thus, the observer matrix reduces to the observer vector $\boldsymbol{c} = \begin{bmatrix} 0 & 0 & 0 & 0 & 0 & 1 \end{bmatrix}$, i.e. $y = \boldsymbol{c} \cdot \boldsymbol{z} = x_3$.

2.2. Linear Quadratic Regulator

The examined system is a single variable system with input $u = F_r$ and disturbance $u_S = F$. For specifying the parameters of the controller in the state space approach an optimal Linear Quadratic Regulator (LQR) is used. The structure of the state controlled system is shown in Fig. 4.
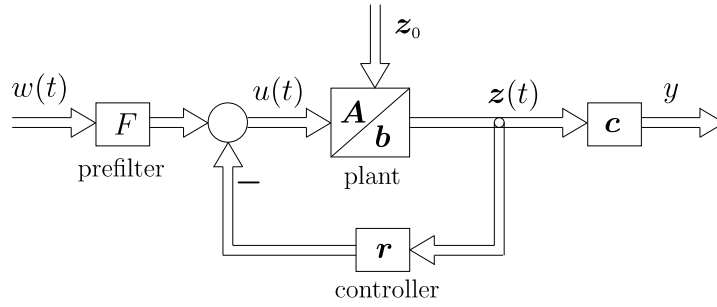
Figure 4. State control[7].

With the controller force becoming

$$F_r = -\boldsymbol{r}^T \boldsymbol{z} \tag{7}$$

the constant gain $\boldsymbol{r}$ of the linear state feedback is sought such that the quadratic cost functional

$$J = \frac{1}{2} \int_0^\infty \left[\boldsymbol{z}^T(t)\boldsymbol{Q}\boldsymbol{z}(t) + \frac{1}{\kappa}F_r^2 \right] dt \tag{8}$$

is minimized with κ being positive and $\boldsymbol{Q}$ being a positive semi-definite matrix. The solution of this minimization problem is

$$\boldsymbol{r} = \kappa\, \boldsymbol{b}^T \boldsymbol{P} \tag{9}$$

with $\boldsymbol{P}$ being the unique positive definite solution of the algebraic RICCATI equation[7, 8]

$$\boldsymbol{P}\boldsymbol{A} + \boldsymbol{A}^T \boldsymbol{P} + \boldsymbol{Q} - \kappa\, \boldsymbol{P}\, \boldsymbol{b}\boldsymbol{b}^T \boldsymbol{P} = 0. \tag{10}$$

The scalar κ is a measure for the cost of the controller input[9], the matrix $\boldsymbol{Q}$ is chosen such that the product $\boldsymbol{z}^T \boldsymbol{Q} \boldsymbol{z}$ represents a modified potential and kinetic energy of the system. With $\boldsymbol{z}^T = [\dot{\boldsymbol{x}}^T, \boldsymbol{x}^T]$ it reads

$$\boldsymbol{Q} = \begin{bmatrix} w_{kin}\boldsymbol{M} & \boldsymbol{0} \\ \boldsymbol{0} & \boldsymbol{C} + \boldsymbol{C}^* \end{bmatrix}. \tag{11}$$

The scalar w_{kin} is a measure for the weighting of the kinetic energy within the quadratic cost function (8). The higher w_{kin} is set, the higher the motion of the system is considered in the setting of the controller parameters. Thus, it is a measure of the damping properties of the controller.

Using the matrix $\boldsymbol{C^*}$, the positioning of the three bodies of the system can be influenced. In the system considered, the position x_3 of mass m_3 is the controlled variable. Thus, the matrix is set to

$$\boldsymbol{C^*} = \begin{bmatrix} 0 & 0 & 0 \\ 0 & 0 & 0 \\ 0 & 0 & C^* \end{bmatrix} \tag{12}$$

with the scalar weight C^*. For $w_{kin} = 1$ and $C^* = 0$, the product $\boldsymbol{z^T Q z}$ actually equals the total energy of the system.

2.3. Simulation Results

The represented results are shown for different values of w_{kin} and C^*, each modifying the matrix $\boldsymbol{Q}$, the corresponding cost function (8), and therefore the controller matrix $\boldsymbol{r}$. To examine the damping of the controller, the system damping is set to zero during all simulations, i.e. $\boldsymbol{D} = (d_{ij}) = 0$. The initial conditions of the system are zero velocities and positions $x_i = 0$. It is disturbed by the external force

$$F = 2\text{kN} \cdot \sigma(t - 0.05\text{s}). \tag{13}$$

In Fig. 5, the influence of w_{kin} on the position x_3 is depicted. For $w_{kin} = 1$, there is only very small damping and the system is oscillating about a mean value x_m, which can be calculated by

$$x_m = \frac{F}{c_{tot}} = F\left(\frac{1}{c_1} + \frac{1}{c_2} + \frac{1}{c_3}\right). \tag{14}$$

It easily can be seen that for increasing w_{kin} the damping of the system increases as well, such that x_3 converges to a limit value $x_e \neq 0$. This limit is a measure for the remaining control error.

Fig. 6 shows the influence of C^* on the controller effect. For these simulations $w_{kin} = 1e5$ is set, thus the damping effect described above occurs. An increase of C^* leads to two results. It increases the damping of the system similarly to an increase of w_{kin}, but it also reduces the remaining control error.
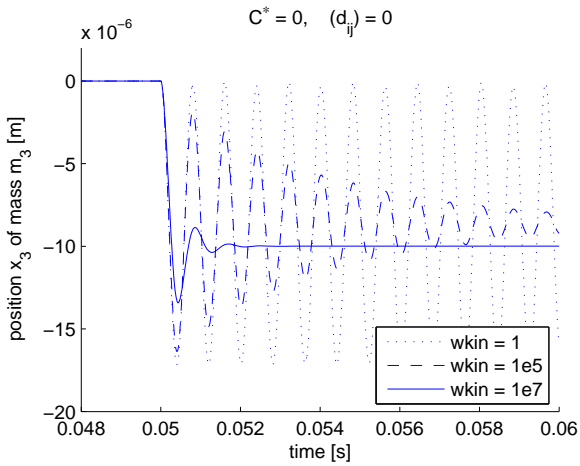
Figure 5. Influence of w_{kin}, with $C^* = 0$.
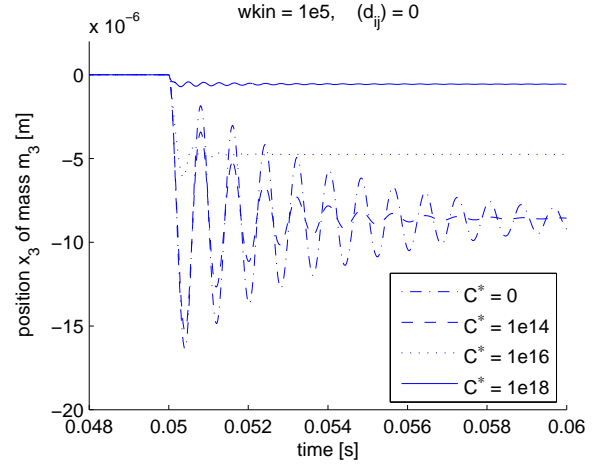
Figure 6. Influence of C^*, with $w_{kin} = 1e5$.

To achieve a zero steady-state error, an additional controller system has to be implemented. In Fig. 7, a possible set-up including an output feedback is shown. The state controlled system $(\boldsymbol{A, b, c, r})$ presented above can be rewritten as a new system with $(\boldsymbol{A^*} = \boldsymbol{A} - \boldsymbol{b} \cdot \boldsymbol{r}, \boldsymbol{b}, \boldsymbol{c})$. It is represented by the transfer function block G. In the feedback path, H is a simple integrator, representing a sensing element, and in the forward path, C is a proportional element. The prefilter F is set to one.
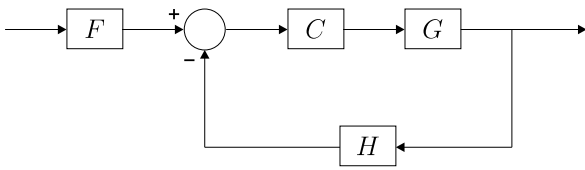
Figure 7. Closed loop system structure with integrator in feedback and proportional element in forward path.
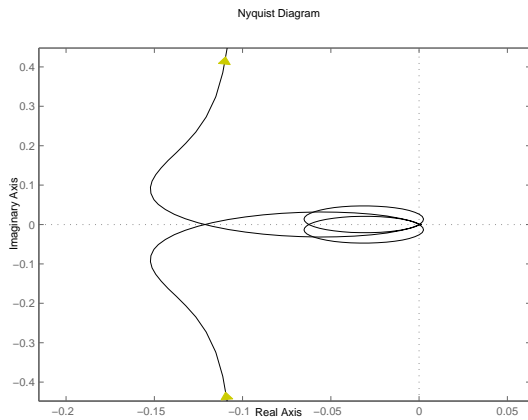
Figure 8. NYQUIST contour of open loop with integrator and proportional element, stability margin.
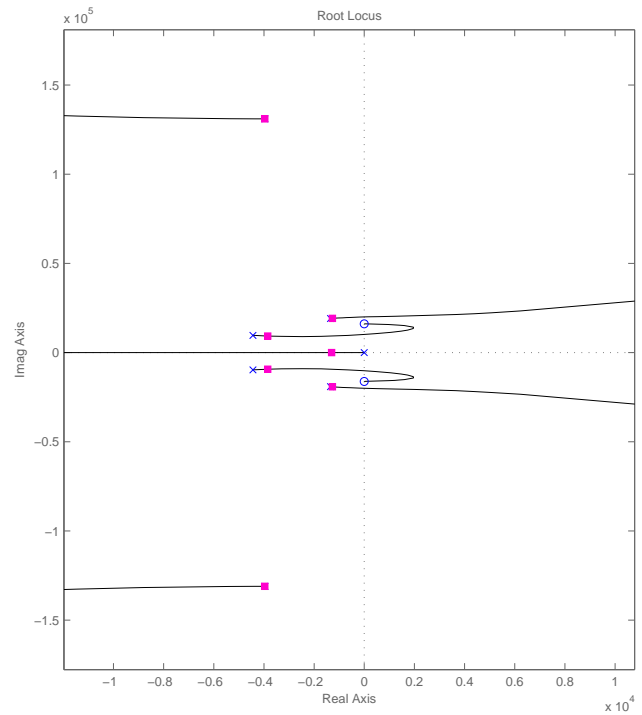
Figure 9. Root locus of closed loop with integrator and proportional element, position of roots for C=1e12.

Using the root locus procedure for a closed loop system[10], an optimal value for the proportional element P can be achieved. The root locus of the examined system is shown in Fig. 9. For $C = 1e12$, an optimal system behavior is achieved with dominating zeros far away from the imaginary axis. The large stability margin of the closed loop according to the NYQUIST criterion can be seen in the NYQUIST contour of the open loop, depicted in Fig. 8. The efficiency of using both controllers is shown in Fig. 10. The maximum deflection of x_3 is less than in most cases of single use of the LQR state controller and there is no remaining steady-state error.
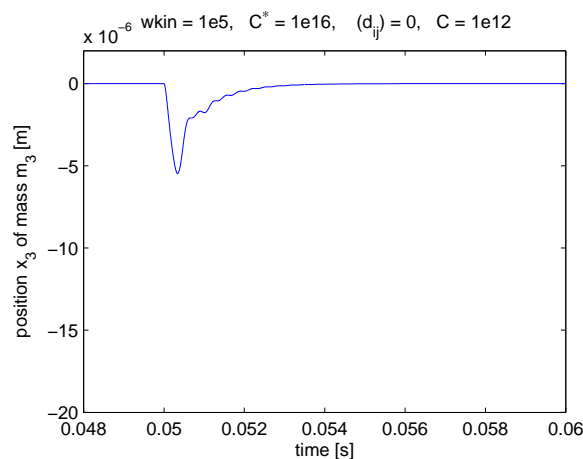
Figure 10. Use of LQR state controller in combination with PI feedback controller.

3. TRANSFER INTO NUMERICAL MODEL

Additionally, the oscillator system shown in Fig. 3 was modeled using the multi-body software MSC.ADAMS, building the basis for the implementation of the flexible adaptronic strut into the complete model of the machine tool with parallel kinematics. To implement the developed control concept described above, the interface to the control software MATLAB/SIMULINK was used. During the simulation, however, the complete state vector $\boldsymbol{z}$, necessary for the application of the state controller, is unknown.

3.1. Full State Observer (Luenberger Observer)

To estimate the complete state vector $\boldsymbol{z}$ of the examined system $(\boldsymbol{A}, \boldsymbol{b})$ and the output measurement y, a LUENBERGER observer is introduced. With observer feedback vector $\boldsymbol{\ell}$, the state vector can be approximated by

$$\dot{\hat{\boldsymbol{z}}} = \boldsymbol{A}\hat{\boldsymbol{z}} + \boldsymbol{b}u + \boldsymbol{\ell} \ (\hat{y} - y). \tag{15}$$

According to Föllinger[7], the eigenvalues of the closed-loop system $(\boldsymbol{A}, \boldsymbol{b})$ are not shifted if an observer is implemented into the system. Their number is simply enhanced by the number of eigenvalues of the observer. As long as the plant is observable and controllable, the eigenvalues of both, controller and observer, can be set separately. Since the considered system is both observable and controllable, applying this *separation theorem* is valid. Finally, it must be ensured that the designed observer is faster than the controller. Thus, the observer poles must be placed further on the left of the imaginary axis than the closed-loop poles[7]. The evaluated eigenvalues for the controlled closed-loop system are listed in Tab. 1. Using the pole placement procedure according to J. Ackermann[7], the poles for the observer are set as listed in Tab. 2, resulting in the observer feedback vector $\boldsymbol{\ell}$ in eq. (15).

$\lambda_{1,2}$	$-3.959e3 \pm 1.31e5i$
$\lambda_{3,4}$	$-1.345e3 \pm 1.91e5i$
$\lambda_{5,6}$	$-4.437e3 \pm 9.66e5i$

Table 1. Eigenvalues of $\boldsymbol{A}^* = \boldsymbol{A} - \boldsymbol{b} \ \boldsymbol{r}$.

$\lambda_{1,2}$	$-4.97e4 \pm 166i$
$\lambda_{3,4}$	$-5.00e4 \pm 333i$
$\lambda_{5,6}$	$-5.03e4 \pm 167i$

Table 2. Eigenvalues of $\boldsymbol{L}^* = \boldsymbol{A} - \boldsymbol{\ell} \ \boldsymbol{c}$.

3.2. Co-Simulation Model

The resulting block diagram with controller, observer and plant is shown in Fig. 11. Controller 1 is the proportional element, controller 2 is the integrator. The state controller contains the control vector $\boldsymbol{r}$ determined in section 2. The disturbance onto the system is described within the external load block, the ADAMS model contains the plant and its interface. The data exchange interval between the two software programs is set to $t = 0.1$ms, identical to the maximum integration step size.
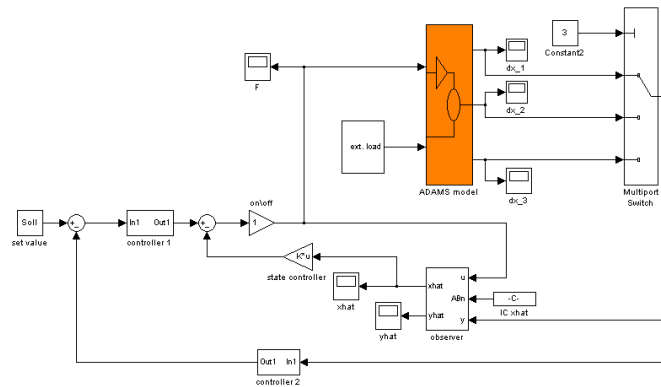
Figure 11. MATLAB/SIMULINK block diagram for co-simulation with MSC.ADAMS.

3.3. Simulation Results

The parameters of the controller used for the co-simulation are determined according to the LQR method described in section 2. The chosen settings are: $w_{kin} = 1e5$, $C^* = 1e16$, $C = 1e12$ and no damping of the system, i.e. $\boldsymbol{D} = (d_{ij}) = \boldsymbol{0}$. Like in the analytical study, the system is excited by the external disturbance described by (13). In Fig. 12 the simulation results of the controlled system are presented. A steady-state error occurs, if solely the LQR state controller is used. This control error can be resolved by switching on the PI control element. In comparison with the simulation results of the analytical description, the maximum deflection of x_3 is larger when both controllers are used. The same holds for the steady-state error for the sole use of the LQR controller. Since the required observer is faster than the state controller, this behavior might solely be a result of the non-variable exchange step size of the co-simulation.

The performance of the designed observer during this simulation is depicted in Fig. 13.
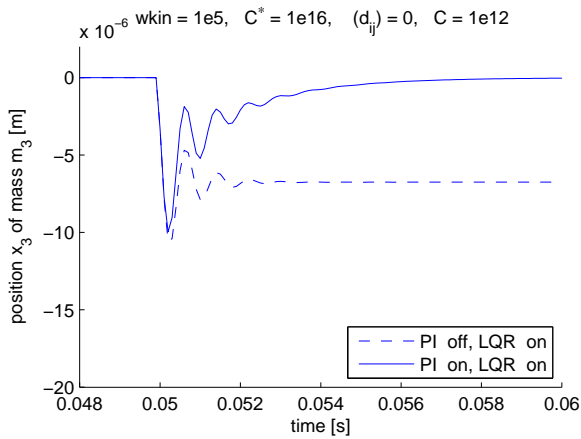
Figure 12. Msc.Adams-Matlab/Simulink cosimulation: influence of LQR controller and PI feedback controller on control variable x_3.
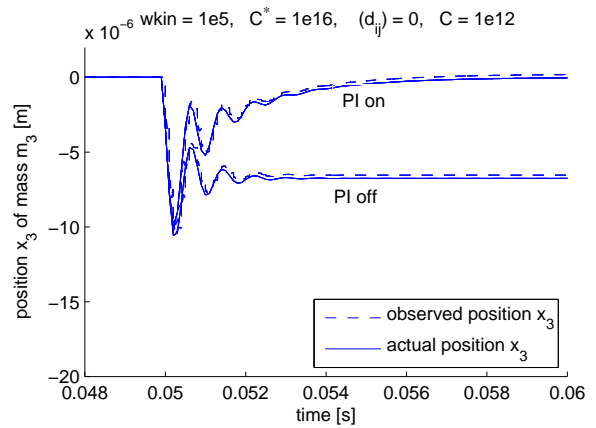
Figure 13. Comparison of position $\hat{y}$ estimated by the observer with actual position $y = x_3$.

4. IMPLEMENTATION OF ADAPTRONIC STRUTS INTO MACHINE TOOL

After finishing the design of the controller for the three-body oscillator, the concept must be transferred onto the complex flexible multi-body model of the adaptronic strut shown in Fig. 14. This procedure was chosen since

Figure 14. Msc.Adams flexible multi-body model of the adaptronic strut.
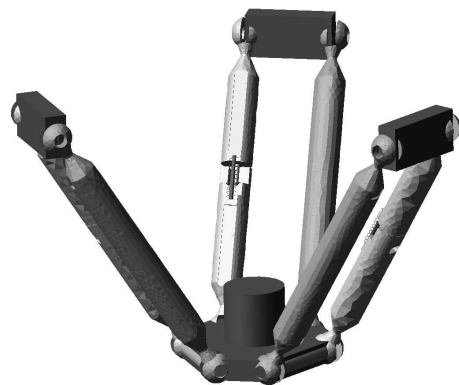
Figure 15. Msc.Adams model of examined machine tool with adaptronic struts at positions 2,3,5 (ad235).

the development of a separate, perfectly fitting control concept for this flexible multi-body model of the strut is rather extensive: The large number of modal coordinates required for describing the flexible behavior of the struts lead to a big quantity of state variables making the handling costly and expensive.

Eventually, the strut must be implemented into the machine tool, as exemplarily shown in Fig. 15 for three adaptronic struts. Both, the compensation efficiency as well as the mechanical behavior of the machine tool, depend on number and position of the substituted struts. Furthermore, the machining process, e.g. drilling or milling, as well as the location within the machine workspace during these processes, influence the decision about number and position of struts.

In a first step, the influence of the stiffness of the machine tool depending on number and position of the exchanged adaptronic struts is examined. The frequency response G_{xx} of the TCP to a process load is depicted in Fig. 16. The implementation of an adaptronic strut reduces the lowest resonance frequencies of the machine tool due to a decrease of its stiffness. The number of the exchanged struts influences the stiffness only marginally, as long as only one strut of a pair per guiding skid is substituted.
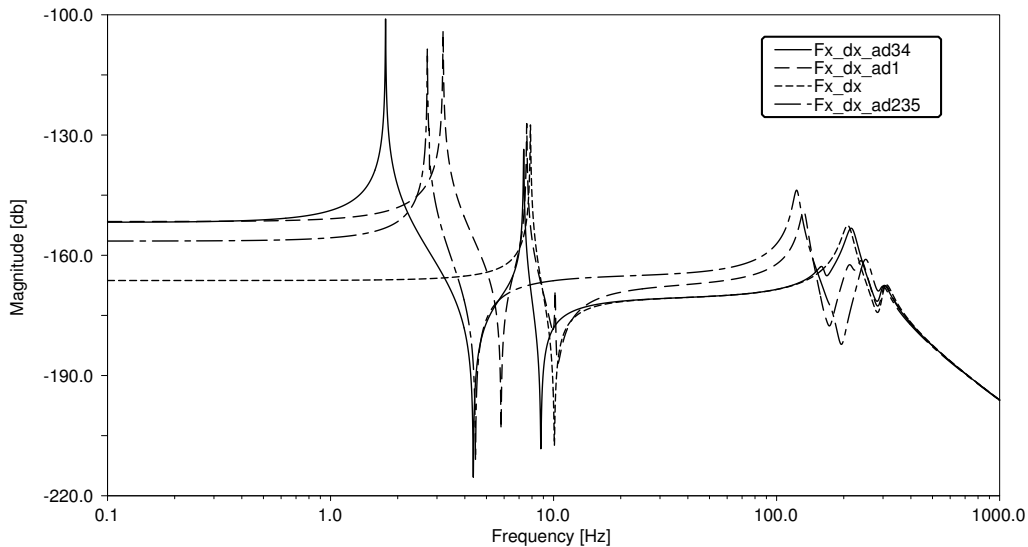
Figure 16. Influence of number and position of adaptronic struts onto the stiffness of the machine tool, shown exemplarily by the frequency response G_{xx} of the position of the TCP to a process load.

5. CONCLUSIONS AND OUTLOOK

In this contribution a control concept for a reduced model of an adaptronic compensation unit for machine tools with parallel kinematics has been presented. With a combination of an optimal state controller and a feedback PI controller the influence of external stepwise static disturbances can be abolished. Thus, the concept is applicable for compensation of static and quasi-static errors within machine tools. For estimating the complete state vector for the use of the state controller a Luenberger observer was established and implemented in a co-simulation model. To determine the influence of number and position of the adaptronic struts on the behavior of the machine tool, a frequency response analysis has been made.

Intended future studies include the control of one or more adaptronic struts within the machine tool. The extension of the single variable control to a multivariable control is essential. Depending on the position of the tool center point in the workspace, the compensation of (quasi-)static errors shall be achieved. Furthermore, machining processes such as drilling and milling shall be considered. An extension of the frequency domain required for compensation might be necessary for this purpose.

ACKNOWLEDGMENTS

REFERENCES

1. C. Rudolf, J. Wauer, J. Fleischer, and C. Munzinger, "An approach for compensation of geometric faults in machine tools", *Proc. IDETC/CIE Conference, ASME* (DETC2005-84241), 2005.
2. C. Rudolf, J. Wauer, J. Fleischer, and C. Munzinger, "Measuring static and slowly changing loads using piezoelectric sensors", *Proc. 10th Int. Conference on New Actuators* (P015), pp. 540–543, 2006.
3. J. Fleischer, A. Knödel, C. Munzinger, and M. Weis, "Designing adaptronical components for compensation of static and quasi-static loads", *Proc. IDETC/CIE Conference, ASME* (DETC2006-99461), 2006.
4. K. Kuhnen, *Inverse Steuerung piezoelektrischer Aktoren mit Hysterese-, Kriech- und Superpositionsopera-toren*, SHAKER-Verlag, 2001.
5. K. Kuhnen and H. Janocha, "Inverse feedforward controller for complex hysteretic nonlinearities in smart material systems", *Control and Intelligent System* **29**(3), pp. 74–83, 2001.
6. H. Janocha and K. Kuhnen, "Real-time compensation of hysteresis and creep in piezoelectric actuators", *Sensors & Actuators, Physical A* **79**, pp. 83–89, 2000.
7. O. Föllinger, *Regelungstechnik*, Hüthig, 1994.
8. J. Lunze, *Regelungstechnik 2*, Springer, 2004.
9. A. Preumont, *Vibration Control of Active Structures – An Introduction*, Kluwer Academic Publishers, 2nd ed., 2002.
10. J. Lunze, *Regelungstechnik 1*, Springer, 2005.